

H.A. Ilchuk¹, L.I. Nykyruy², A.I. Kashuba¹, I.V. Semkiv¹, M.V. Solovyov¹,
B.P. Naidych², V.M. Kordan³, L.R. Deva¹, M.S. Karkulovska¹, R.Y. Petrus¹

Electron, Phonon, Optical and Thermodynamic Properties of CdTe Crystal Calculated by DFT

¹Lviv Polytechnic National University, Bandera Str. 12, 79646 Lviv, Ukraine, andrii.i.kashuba@lpnu.ua

²Vasyl Stefanyk Precarpathian National University, Shevchenko Str. 57, 76018 Ivano-Frankivsk, Ukraine,
lyubomyr.nykyruy@pnu.edu.ua

³Ivan Franko National University of Lviv, Kyrylo & Mephody Str. 6, 79005 Lviv, Ukraine

Electronic and phonon band structure, thermodynamic and optical properties are studied for the CdTe crystal. We calculated the electron and phonon dispersion at high symmetry directions, density of electron and phonon state, temperature dependence feature of Raman spectra, heat capacity, free energy, entropy, enthalpy and Debye temperature estimated with the generalized gradient approximation (GGA). A Perdew–Burke–Ernzerhof functional (PBE) was utilized. To study the optical properties was use a complex dielectric function $\epsilon(\hbar\omega)$. All of the calculated parameters correlate well with the known experimental data.

Keywords: density functional theory, band structure, optical functions, thermodynamic properties.

Received 4 February 2022; Accepted 16 May 2022.

Introduction

Cadmium chalcogenides crystals namely CdTe belongs to a large II–VI group of semiconductor compounds. This material is characterized by different degrees of ionic, metallic, covalent bonding, and crystallizes in several crystal structures such as zincblende and wurtzite. CdTe has a melting point 1092 °C [1], and is the most fusible among II–VI group of semiconductor compounds. It crystallizes in the sphalerite structure with $a = 6.481 \text{ \AA}$ [1], which is stable to 1000 K. Each atom of CdTe is located in the center of a regular tetrahedron in which on the tops located the atoms of another element. Wurtzite structure type in purest form in crystals are not obtained, but observed at high pressures and temperatures [2], and in thin film. Lattice parameters of the hexagonal phase are $a = 4.57 \text{ \AA}$, $c = 7.47 \text{ \AA}$ [1]. CdTe possess the high density of 5.85 g/cm^3 and a sharp absorption edge and high efficiency of light absorption of around 90 % [3]. CdTe bandgap E_g is 1.531 eV at $T = 300 \text{ K}$ and 1.608 eV at $T \approx 0 \text{ K}$ [4]. Its Zinc blende symmetry possesses a high electro-optical coefficient r_{41}

that can be used in efficient Pockels cell. r_{41} coefficient for CdTe is about three times higher than for InP or GaAs in the infrared part of the electromagnetic spectrum [5].

Cadmium telluride (CdTe) of considerable technological importance for many purposes, such as photovoltaics [6-9], medical imaging [10], electro-optic modulators, photorefractive systems, photodetector [11], thermoelectric [12]. CdTe can show both n -type and p -type electrical conductivity which can be used in diodes and transistors. Cadmium telluride composed of two elements cadmium Cd ($Z = 48$) and telluride Te ($Z = 52$), which high effective atomic number $Z_{\text{eff}} = 50$ is essential for the good attenuation of up to several hundred keV of ionizing radiation. Also CdTe has high mobility-lifetime product ($\mu\tau$). Thus CdTe is a very attractive material for X- and γ -radiation detection with many advantages over other semiconductors [13, 14]. According to the Shockley-Quessier limit [15], the maximum power conversion efficiency (PCE) of cadmium telluride is up to 32 %, which is a promising material for photovoltaic applications. CdTe has a direct band gap of 1.5 eV at room temperature and a high light absorption coefficient (over

10^4 cm^{-1}) which are the optimal for solar light collection and makes compound to be an attractive material for solar cell applications [16-19] which also characterized low manufacturing.

The structural and electronic properties of cadmium telluride are being investigated, both experimentally and theoretically during the many years. Theoretical studies were conducted by the *ab initio* calculations and have been extensively used to carry out the structural [20], electronic [21, 22], elastic [23], thermodynamic [24], optical [25, 26] and lattice dynamical [24] properties for cadmium chalcogenides. In [27, 28] calculations of structural and electronic properties was performed using standard LDA/GGA and the hybrid functional (HSE06). In addition to calculations of the band structure DFT are used to establish the optical and thermodynamic parameters of cadmium telluride but with different approaches: by B3LYP hybrid functional [29]; all-electron full potential linearized augmented plane wave method [12]. Some properties of CdTe namely electronic and optical properties were calculated under hydrostatic pressure [30, 31]. However, in different articles use different approaches that gives some discrepancies, for example for band gap value, with the experimental data and with each other.

In this work, we report on the fundamental electron and phonon properties of the CdTe crystal. Having performed the electronic band-structure calculations for CdTe, one can obtain their optical parameters. Finally, we have derived the temperature dependence of Raman spectra, free energy, heat capacity, entropy, enthalpy and Debye temperature.

I. Methods of calculation

The theoretical calculations were performed within the framework of the density functional theory (DFT). To calculate the properties of single-crystalline CdTe, a crystalline lattice with the basal parameters given below was used. To describe the exchange-correlation energy of the electronic subsystem, a functional in the approximation of generalized gradient (GGA) and the Purdue–Burke–Ernzerhof (PBE) parameterization [32] was used. As a correlation potential, the Ceperlay–Alder and Gell–Mann–Brueckner equations were applied to the high electron-density boundaries.

The charge-density distribution was calculated by the method of special points involving the techniques of charge damping. The relaxation of ion positions on the basis of calculated atomic forces was achieved for each crystal structure, and then the integral stress of the cell was determined.

The value $E_{\text{cut-off}} = 660 \text{ eV}$ for the energy of cutting-off the plane waves was used in our calculations. The electron configurations $4d^{10}5s^2$ for Cd and $5s^25p^4$ for Te atoms formed the valence electron states. The integration over the Brillouin zone (BZ) was performed on the $4 \times 4 \times 4$ grid of k points using the Monkhorst–Pack scheme [33]. The self-consistent convergence of the total energy was taken as $5.0 \times 10^{-6} \text{ eV/atom}$. For DFT calculations of CdTe crystal the $3 \times 3 \times 3$ supercell containing 256 atoms has been created. The cubic structure has been used for the

optimized structure of the crystal supercell $\text{Cd}_{16}\text{Te}_{16}$. Geometry optimization of the lattice parameters and atomic coordinates were performed using the Broyden–Fletcher–Goldfarb–Shanno (BFGS) minimization technique with the maximum ionic Hellmann–Feynman forces within 0.01 eV/\AA , the maximum ionic displacement within $5.0 \times 10^{-4} \text{ \AA}$, and the maximum stress within 0.02 GPa . These parameters are sufficiently small to lead to a well-converged total energy of the structures studied.

The energy band diagram was constructed using the points of the BZ in the inverse space, which were as follows: X(0.5, 0, 0.5), R(0.5, 0.5, 0.5), M(0.5, 0.5, 0) and G(0, 0, 0).

II. Results and Discussion

2.1. Electron band energy structure

The full energy band diagrams of the CdTe crystal is shown along the highly symmetric lines of the tetragonal BZ in fig. 1. The energy in this case is counted from the Fermi level. Analysis of the results of theoretical calculations of the energy band spectrum shows that the smallest bandgap is localized in the center of the BZ (the point G).

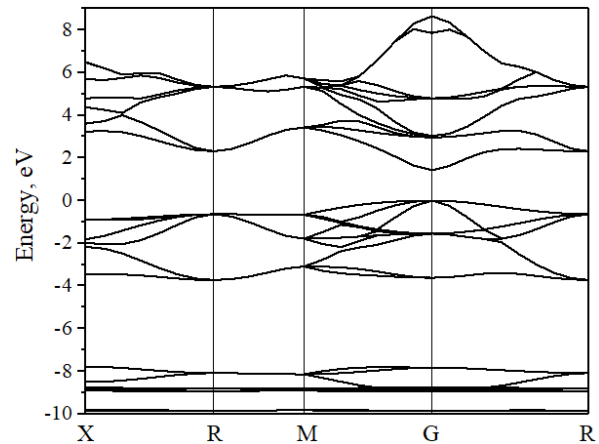


Fig. 1. Electron band energy structure of CdTe crystal.

This means that the crystal is characterized by a direct energy bandgap. Our bandgap E_g prove to be less than the appropriate parameters derived experimentally for pure CdTe ($\sim 1.44 \text{ eV}$ [26]) crystal. Note, however, that the generalized gradient approximation always suffers from unavoidable underestimation of the bandgap (see Table 1).

Table 1

Comparison of experimental and calculation basic physical properties for CdTe crystal.

Parameters	Calculation value	Experimental value
$a, \text{ \AA}$	6.564376	6.4765(19) [22]
$B, \text{ GPa}$	45.13	39 [38]
$E_g, \text{ eV}$	1.418	1.44 [26]

The underestimation of the bandgap is a known issue with this calculation approach. The easiest way to get the results closer to experimental ones is to use a so-called

‘scissor’ operator, which leads to changing the bandgap by shifting the conduction band into the region of higher energies. This operator is based on the proximity of the $E(k)$ dispersion dependences of the energies of conduction bands, which are determined from the Kohn–Sham equations [34]. The conduction bands of the calculated energy spectrum are usually shifted until the experimental value of the minimum energy gap bandwidth E_g of the crystal is achieved. In this work, the calculated value was corrected to the value of $\Delta E = 0.022$ eV for CdTe to bring the absolute E_g values into agreement. However, this does not affect the overall trend in the electronic and structural properties, which is confirmed by a number of previous calculations of the electronic states [35, 36].

The analysis of partial contributions of individual levels to the function of the total density of states (Fig. 2) and the partial contributions of individual bands to the electronic density allows us to find genesis of the valence and conduction bands for the CdTe crystal. The lowest band near -10 eV is formed by the s states of Te. The following bands dispersed at the energy marker near -9 eV is formed because of the contributions of the d states of Cd. The peak of the valence complex is practically formed by the p states of Te, with ‘contamination’ of the p states of Cd. But the conduction band bottom is mainly formed by the p states of Cd and Te, as well as by the s states of Cd.

Basically, the physical properties of compounds are determined by the nature of chemical bonds and the peculiarities of the electronic structure. An effective indicator of charge distribution is the spatial map of electron density distribution [37]. The charge density contour diagrams in planes along the internuclear axis for the CdTe crystals are represented in Fig. 3.

The mixed ionic-covalent nature of the bond in the CdTe compound determines the distribution of charge regions around atomic backbones. Almost the same size electron clouds around the atoms are connected by a fairly wide "bridge", which indicates the covalent nature of such a bond. The concentration of higher electron density near the metal atom is observed due to the consideration of d -states and weakly held bonding electrons.

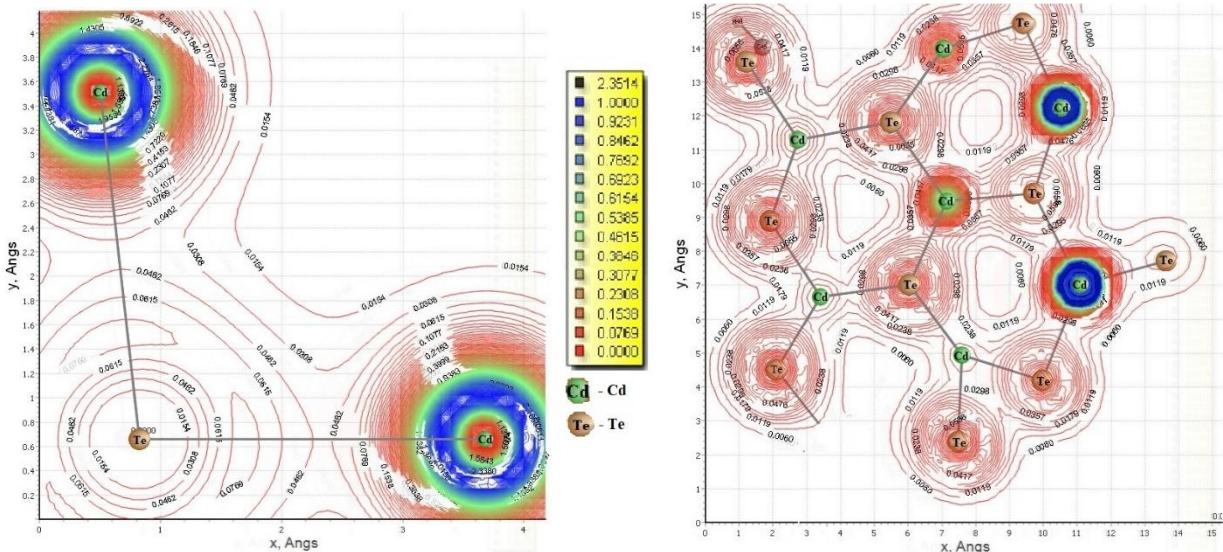


Fig. 3. Charge density contour diagrams in CdTe crystals.

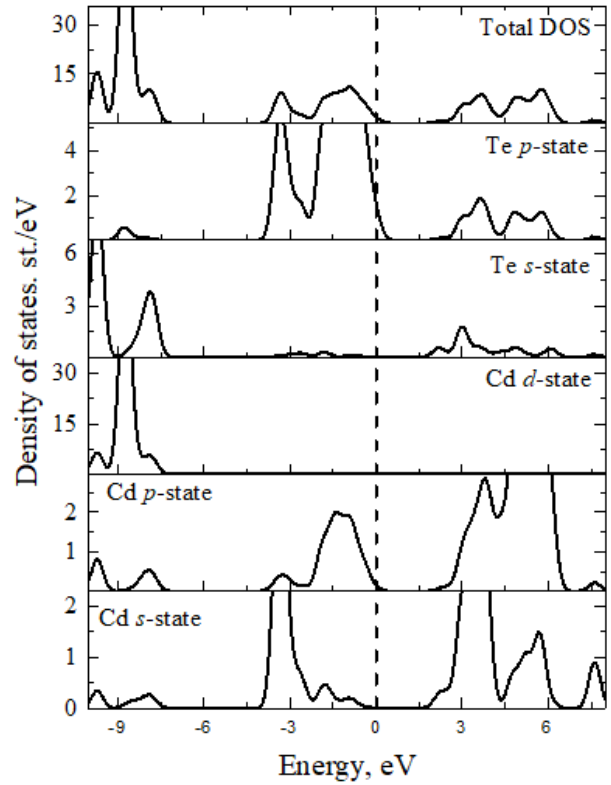


Fig. 2. Electron density of states of CdTe crystal.

2.2. Phonon band energy structure

The curves of phonon dispersion ω_p and total phonon density of states of CdTe at several high symmetry BZ points are represented in Fig. 4. As it has been known [22], a crystal lattice consisting of four atoms per unit cell has $12(3 \times 4)$ branches in which three of them are acoustic and the rest are optical. It can be seen that 3 acoustic branches

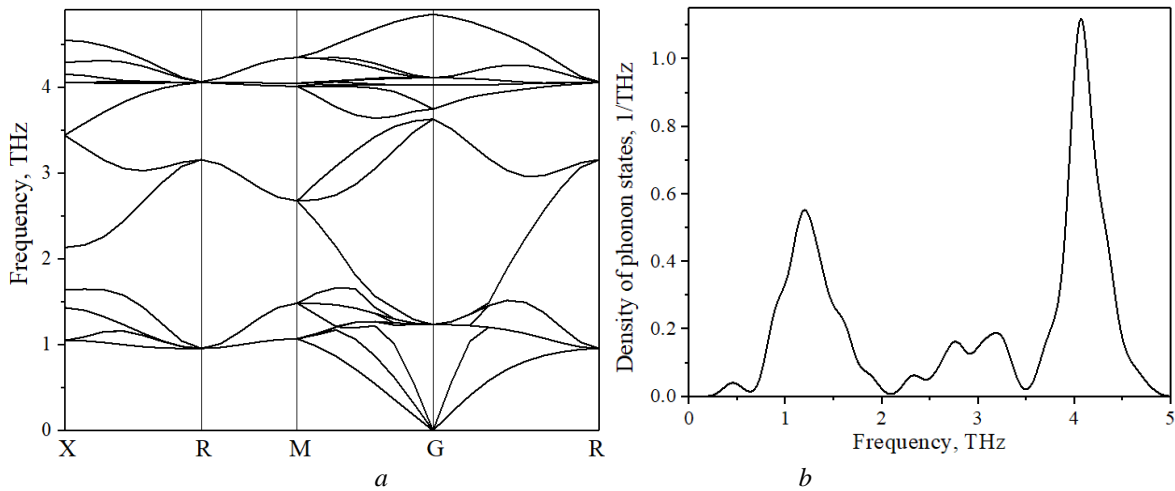


Fig. 4. The phonon dispersion ω_p curves (a) and total phonon density of states (b) of CdTe crystal.

Table 2

The phonon frequencies (in THz) for CdTe at 300 K.

Mode	TO(G)		LO(G)		LA(G)	TA(G)	TO(X)	TA(X)
This work	4.11		4.85		0	0	4.30	1.05
Reference	4.17 [39]	4.20 [38]	5.01 [39]	5.08 [38]	0 [38]	0 [38]	4.44 [38]	1.05 [38]

that correspond to sound propagation as $q \rightarrow 0$ and 9 optical branches emerge from point G (with $\omega=0$). The acoustic modes are including the longitudinal acoustic (LA) and transverse acoustic (TA) modes. The highest phonon frequency of ~ 4.85 THz was found at point G.

corresponding to vibrational modes of crystal structural elements were observed in the frequency range $80 - 180 \text{ cm}^{-1}$ at different temperatures $0.1 - 1000 \text{ K}$. RS are shows single peak localization near 134 cm^{-1} . This peak was increases with increasing temperature (see Fig. 6).

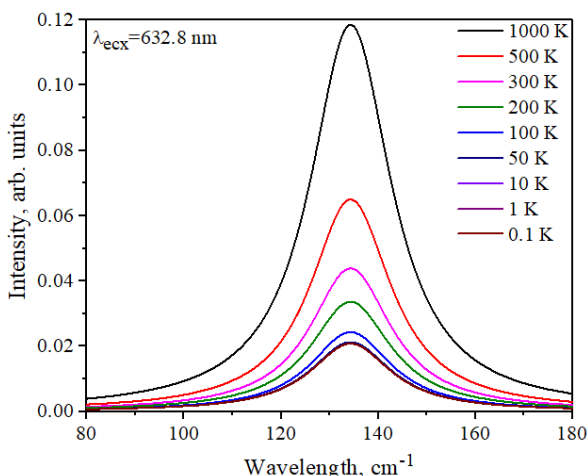


Fig. 5. RS of CdTe crystal at different temperatures.

Phonon frequencies calculated at the high-symmetry points are also listed in Table 2. Along the symmetry direction $G \rightarrow R$ ($G \rightarrow M$), the TO branch is gradually increasing amount of upward dispersion, but LO branch is decreasing. They note that the values for the longitudinal and transverse optic modes of 4.85 and 4.11 THz, respectively, are in good agreement with the values given in Ref. [39].

Fig. 5 shows theoretically calculated Raman scattering (RS) spectra of CdTe crystal at different temperatures between 0.1 and 1000 K. Series of peaks

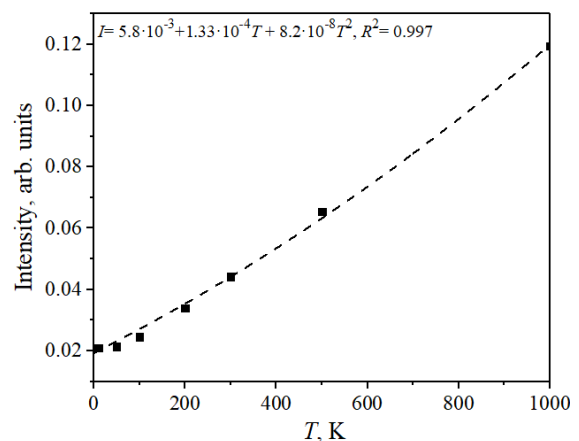


Fig. 6. Temperature dependence of intensity of the band at RS (134 cm^{-1}) for CdTe crystal. Legend: dashed line – functions of approximation, R^2 – determination coefficient.

Temperature dependence of Raman active bands shows parabolic behavior and don't shifted position with increasing temperature (see legend on Fig. 6). The calculated RS spectra agreed well with the experimental ones although peaks were slightly shifted (139 cm^{-1} [40]). This could be due to specifics of DFT theory. The theoretical calculations found that Cd–Te symmetric stretching modes contributed most to vibration in RS at the frequency 134 cm^{-1} (see Fig. 7).

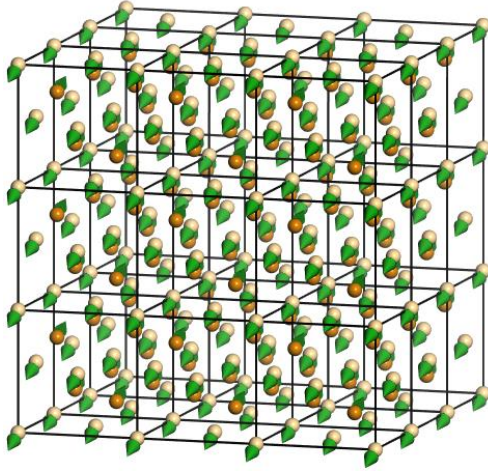


Fig. 7. Vibrations in the CdTe (at 134 cm^{-1}) crystal (Light balls – Cd, brown balls – Te).

2.3. Optical properties

To study the optical properties, it is convenient to use a complex dielectric function $\varepsilon(\hbar\omega)$. The imaginary part of the dielectric function $\varepsilon(\hbar\omega)$ ($\varepsilon = \varepsilon_1 + i\varepsilon_2$) for CdTe crystal (Fig. 8) can be calculated using the relation (1). Then the real part of the $\varepsilon_1(\hbar\omega)$ function can be obtained from the Kramers–Kronig relation (2).

$$\varepsilon_2 = \frac{2e^2\pi}{V\varepsilon_0} \sum_{k,v,c} |\langle \Psi_K^c | \hat{u} \cdot r | \Psi_K^v \rangle|^2 \delta(E_K^c - E_K^v - \hbar\omega) \quad (1)$$

$$\varepsilon_1 - 1 = \frac{2}{\pi} \int_0^{\infty} \frac{t\varepsilon_2(t)dt}{t^2 - (\hbar\omega)^2} \quad (2)$$

As seen from the curve of the imaginary part of the dielectric function, the first critical point of the dielectric function in the form of fundamental absorption edge arises at an energy level of about 1.4 eV. With increasing energy, a typical rapid increase in the $\varepsilon_2(\hbar\omega)$ value is observed [22]. We can observe a significant anisotropy of the dielectric function that varies with the optical polarization (see Fig. 8).

Using the calculated spectra for the real (Eq. (2)) and imaginary (Eq. (1)) parts of the dielectric function, one can obtain the following spectral dependences of the refractive index (n) and extinction coefficient (k):

$$n = \sqrt{\frac{(\varepsilon_1^2 + \varepsilon_2^2)^{1/2} + \varepsilon_1}{2}}, \quad k = \sqrt{\frac{(\varepsilon_1^2 + \varepsilon_2^2)^{1/2} - \varepsilon_1}{2}}, \quad (3)$$

The theoretical dependence of the refractive index for CdTe in the visible region of the spectrum is shown in Fig. 9. We obtained $n = 2.61$ at $\lambda = 10.6 \mu\text{m}$, if comparisons this value with known data from literature ($n = 2.672$ [39] and $n \approx 2.81$ [41] at $\lambda = 10.6 \mu\text{m}$) can be see good agreement. The refractive indices obtained theoretically are less than the experimental ones, which can be caused by the negative contribution of infrared absorption in the crystal, which has not been taken into account in the calculations. Using the calculated spectra of

the real and imaginary parts of the dielectric function (see Fig. 8), the spectral dependences of the optical conductivity (σ) can be obtained (Fig. 10):

$$\sigma = \sigma_1 + i\sigma_2 = -i \frac{\omega}{4\pi} (\varepsilon - 1), \quad (4)$$

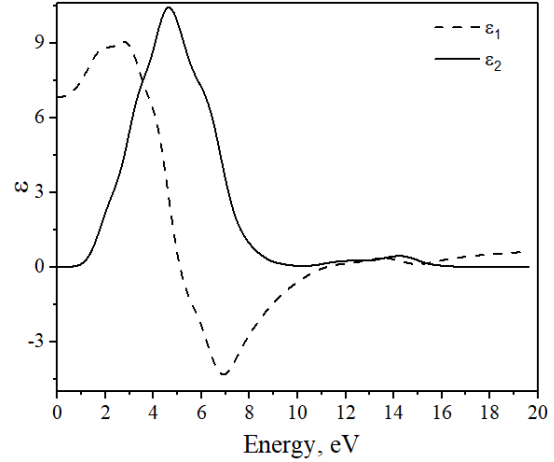


Fig. 8. Real (a) and imaginary (b) components of dielectric function ε calculated for CdTe crystal.

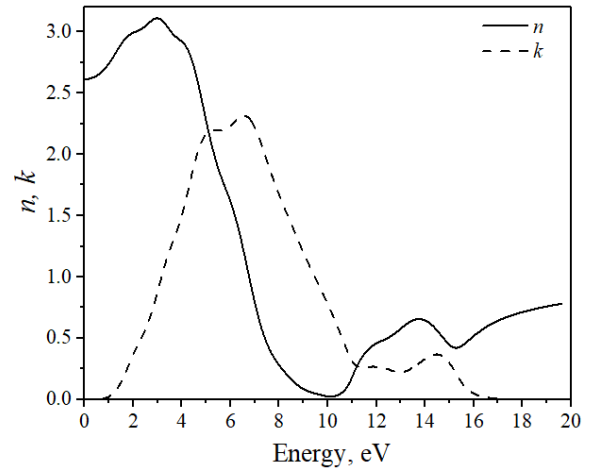


Fig. 9. Theoretically calculated spectra of refractive index (a) and extinction coefficient (b) for CdTe crystal.

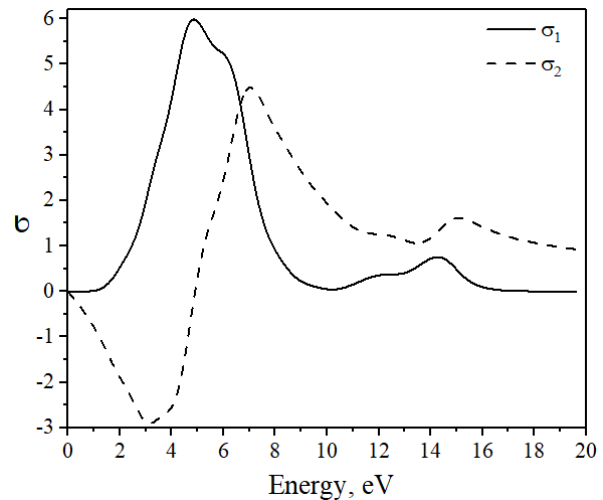


Fig. 10. Real (a) and imaginary (b) components of conductivity σ for CdTe crystal.

2.4. Thermodynamics properties

The estimated temperature dependence features of free energy (F) and enthalpy (E) are presented in Fig. 11. As shows in Fig. 9, free energy (F) is decreases and tends to zero and negative values with increasing temperature, while the enthalpy (E) is increases. The calculated entropy (S) increases upon increasing temperature indicating that by raising temperature, it causes deeper oscillations of crystal planes.

Figure 12 shows the constant-volume specific heat capacity for CdTe. As can be seen at high temperature, it almost approaches the Petit-Dulong limit representing that at high temperature, all phonon modes are motivated by the thermal energy according to the observed behaviors of solids at high temperature [42].

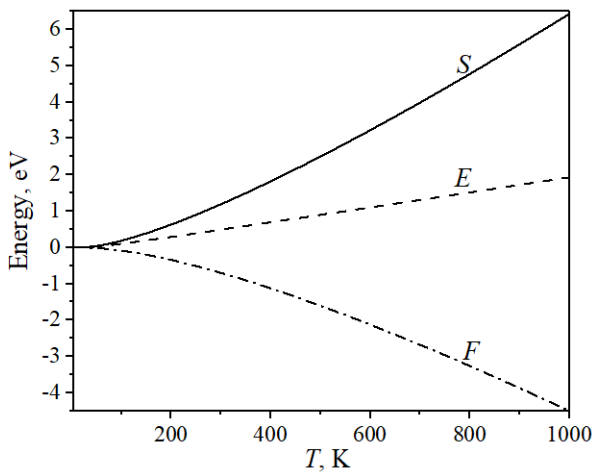


Fig. 11. Calculated temperature dependence (5–1000 K) of free energy (F) and enthalpy (E) and entropy (S) for CdTe crystal.

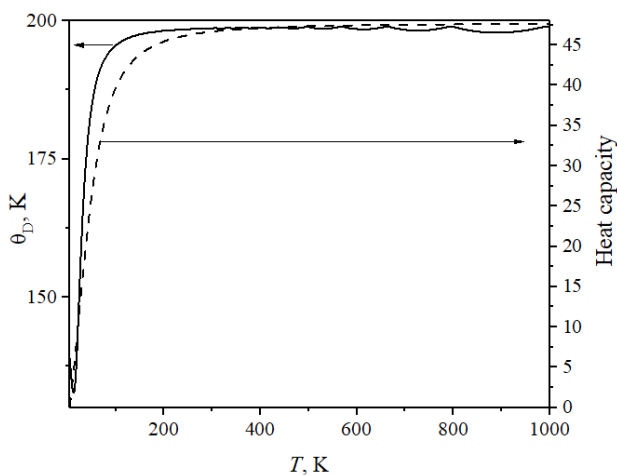


Fig. 12. Calculated temperature dependence (5–1000 K) of Debye temperature for CdTe crystal.

The Debye temperature θ_D is one of the most important parameters that determine thermal properties of a material. The Debye temperature can be defined in terms of the mean acoustic velocity and gives explicit information about the lattice vibrations. This is the highest temperature that corresponds to the highest-frequency normal vibration ν_D , $\theta_D = h\nu_D/k_B$ (where $k_B = 1.380658 \cdot 10^{-23} \text{ J}\cdot\text{K}^{-1}$). At relatively low

temperatures, the vibrational excitations arise mainly due to acoustic oscillations. Notice that the value obtained for the Debye temperature ($\theta_D = 153 \text{ K}$, $T = 25 \text{ K}$) correlates well with the other θ_D values ($\theta_D = 158 \text{ K}$, $T = 25 \text{ K}$) [38].

Conclusion

Basing on the application of a number of modern theoretical approaches, in this work we elucidate a set of results that solve an important scientific and applied problem. The main results of the work reported in the present work can be summarized as follows:

1. First-principle theoretical studies of the electron energy spectrum for the CdTe crystal have been carried out using the reliable techniques of density functional theory and known approximations. It has been established that the smallest bandgap is localized at the center of the BZ (i.e., at the point G). Therefore, our substances should reveal direct optical transitions. We have good agreement of obtained theoretical value of bandgap with known experimental results (1.418 eV).

2. The phonon spectrum and frequencies of atomic vibrations in CdTe crystal were calculated using DFT. It was found that RS spectra calculated *ab initio* agreed rather well with the experimental data. Single peak of RS was observed in crystal which increases with increasing temperature. Temperature dependence of Raman active bands shows parabolic behavior and don't shifted position with increasing temperature.

3. To study the optical properties was use a complex dielectric function $\epsilon(\hbar\omega)$. Using Kramers–Kronig relation was calculation reflective index, extinction coefficient, real and imaginary part of dielectric function and optical conductivity.

4. Free energy is decreases and tends to zero and negative values with increasing temperature, while the enthalpy and entropy is increases, it causes deeper oscillations of crystal planes. At high temperature, all phonon modes are motivated by the thermal energy according to the observed behaviors of solids at high temperature. The value obtained for the Debye temperature correlates well with the other θ_D values.

Hence, the analysis of the fundamental physical properties of CdTe crystal which has been carried out in this work, makes it possible to proceed in the future to large-scale researches (2D and/or 0D structures based on this materials) aimed at producing the devices, which are based on these semiconductor compounds.

Acknowledgments

This work was supported by the Project of Young Scientists 0121U108649 of the Ministry of Education and Science of Ukraine.

Ilchuk H.A. – Sc.D, Profesor at the Department of General Physics;
Nykyruy L.I. – Ph.D, Head of the Department of Physics and Chemistry of Solids;
Kashuba A.I. – Ph.D, Docent at the Department of General Physics;
Semkiv I.V. – Ph.D, Docent at the Department of General Physics;
Solovyov M.V. – Ph.D, Assistant at the Department of General Physics;

Naidych B.P. – Ph.D, Senior Researcher of Department of Physics and Chemistry of Solids;
Kordan V.M. – Ph.D, Research Fellow at the Department of Inorganic Chemistry;
Deva L.R. – Ph.D Student at the Department of General Physics;;
Karkulovska M.S. – Ph.D, Docent at the Department of General Physics;
Petrus R.Y. – Sc.D, Head of the Department of General Physics.

- [1] N.N. Kolesnikov, V.V. Kveder, E.B. Borisenko, D.N. Borisenko, B.A. Gnesin, R.B. James, *Journal of Crystal Growth*. 285(3), 339 (2005); <https://doi.org/10.1016/j.jcrysgro.2005.08.027>.
- [2] S.W. Biernacki, U. Scherz, Ch. Schrepel, *Phys. Rev. B*. 56, 4592 (1997); <https://doi.org/10.1103/PhysRevB.56.4592>.
- [3] Z.R. Khan, M. Zulfeqar, M.S. Khan, Structural, optical, photoluminescence, dielectric and electrical studies of vacuum-evaporated CdTe thin films, *Bull. Mater. Sci.* 35, 169 (2012); <https://doi.org/10.1007/s12034-012-0274-x>.
- [4] K.P. O'Donnell, P.G. Middleton, Bandgaps of widegap II-VIs, temperature dependence, in: R. Bhargara (Eds.), *Properties of Wide Bandgap II-VI Semiconductors* (London, U.K.: INSPEC, Institute of Electrical Engineers, 1997).
- [5] B. Bylisma, P.M. Bridenbaugh, D.H. Olson, A.M. Glass, Photorefractive properties of doped cadmium telluride, *Appl. Phys. Lett.* 51, 889 (1987); <https://doi.org/10.1063/1.98845>.
- [6] A. Munshi, J. Kephart, A. Abbas, J. Raguse, J.-N. Beaudry, K. Barth, J. Sites, J. Walls, W. Sampath, Polycrystalline CdSeTe/CdTe Absorber Cells With 28 mA/cm² Short-Circuit Current, *IEEE Journal of Photovoltaics* 8(1), 310 (2018); <https://doi.org/10.1109/JPHOTOV.2017.2775139>.
- [7] M.A. Green, E.D. Dunlop, J. Hohl-Ebinger, M. Yoshita, N. Kopidakis, X. Hao, Solar cell efficiency tables (version 57), *Prog. Photovolt. Res. Appl.* 29(1), 3 (2018); <https://doi.org/10.1002/pip.3371>.
- [8] T.C.M. Santhosh, K.V. Banger, G.K. Shivakumar, Synthesis and band gap tuning in CdSe_(1-x)Te_(x) thin films for solar cell applications, *Solar Energy* 153, 343 (2017); <https://doi.org/10.1016/j.solener.2017.05.079>.
- [9] X. Zheng, D. Kuciauskas, J. Moseley, E. Colegrove, D.S. Albin, H. Moutinho, J.N. Duenow, T. Ablekim, S.P. Harvey, A. Ferguson, W.K. Metzger, Recombination and bandgap engineering in CdSeTe/CdTe solar cells, *APL Materials* 7, 071112 (2019); <https://doi.org/10.1063/1.5098459>.
- [10] H.B. Barber, Applications of semiconductor detectors to nuclear medicine, *Nucl. Instrum. Methods Phys. Res. A*. 436(1-2), 102 (1999); [https://doi.org/10.1016/S0168-9002\(99\)00605-1](https://doi.org/10.1016/S0168-9002(99)00605-1).
- [11] B.G. Valmik, M.P. Deshpande, S.V. Bhatt, V. Sathe, H.R. Bhoi, P. Rajput, S.H.Chaki, Investigation and fabrication of Cadmium Telluride (CdTe) single crystal as a photodetector, *Physica B: Condensed Matter*. 614, 413027 (2021); <https://doi.org/10.1016/j.physb.2021.413027>.
- [12] J. Mani, N. Rajeev Kumar, R. Radhakrishnan, G. Anbalagan, Thermoelectric properties of CdTe materials: DFT study, *AIP Conference Proceedings* 2265, 030390 (2020); <https://doi.org/10.1063/5.0016968>.
- [13] A. Winkler, H. Koivunoro, V. Reijonen, I. Auterinen, S. Savolainen, Prompt gamma and neutron detection in BNCT utilizing a CdTe detector, *Appl. Radiat. Isot.* 106, 139 (2015); <https://doi.org/10.1016/j.apradiso.2015.07.040>.
- [14] A. Gädda, J. Ott, A. Karadzhinova-Ferrer, M. Golovleva, M. Kalliokoski, A. Winklera, P. Luukka, J. Härkönen, Cadmium Telluride X-ray pad detectors with different passivation dielectrics, *Nucl. Instrum. Methods Phys. Res. A* 924, 33 (2019); <https://doi.org/10.1016/j.nima.2018.08.063>.
- [15] W. Shockley, H.J. Queisser, Detailed Balance Limit of Efficiency of p-n Junction Solar Cells, *J. Appl. Phys.* 32, 510 (1961); <https://doi.org/10.1063/1.1736034>.
- [16] M. Gloeckler, I. Sankin, Z. Zhao, CdTe Solar Cells at the Threshold to 20% Efficiency, *IEEE J. Photovolt.* 3(4), 1389 (2013); <https://doi.org/10.1109/JPHOTOV.2013.2278661>.
- [17] K. Shen, Q. Li, D. Wang, R. Yang, Y. Deng, M.-J. Jeng, D. Wang, CdTe solar cell performance under low-intensity light irradiation, *Sol. Energy Mater. Sol. Cells*. 144, 472 (2016); <https://doi.org/10.1016/j.solmat.2015.09.043>.
- [18] L. Nykyruy, Y. Saliy, R. Yavorskyi, Y. Yavorskyi, V. Schenderovsky, G. Wisz, & S. Górný, CdTe vapor phase condensates on (100) Si and glass for solar cells. In 2017 IEEE 7th International Conference Nanomaterials: Application & Properties (NAP) (IEEE 2017). P. 01PCSI26; <https://doi.org/10.1109/NAP.2017.8190161>.
- [19] L.I. Nykyruy, R.S. Yavorskyi, Z.R. Zapukhlyak, G. Wisz, P.Potera, Evaluation of CdS/CdTe thin film solar cells: SCAPS thickness simulation and analysis of optical properties, *Optical Materials* 92, 319 (2019); <https://doi.org/10.1016/j.optmat.2019.04.029>.

- [20] N. Benkhattou, D. Rached, B. Soudini, M. Driz, High-pressure stability and structural properties of CdS and CdSe, *Phys. Status Solidi B* 241, 101 (2004); <https://doi.org/10.1002/pssb.200301907>.
- [21] E. Deligoz, K. Colakoglu, Y. Ciftei, Elastic, electronic, and lattice dynamical properties of CdS, CdSe, and CdTe, *Physica B* 373, 124 (2006); <https://doi.org/10.1016/j.physb.2005.11.099>.
- [22] H.A. Ilchuk, R.Yu. Petrus, A.I. Kashuba, I.V. Semkiv, and Eh.O. Zmiiovska, Optical-Energy Properties of the Bulk and Thin-Film Cadmium Telluride (CdTe), *Nanosistemi, Nanomateriali, Nanotehnologii* 16(3), 519 (2018); <https://doi.org/10.15407/nnn.16.03.519>.
- [23] R. Wright, J. Gale, Interatomic potentials for the simulation of the zinc-blende and wurtzite forms of ZnS and CdS: Bulk structure, properties, and phase stability, *Phys. Rev. B* 70, 035211 (2004); <https://doi.org/10.1103/PhysRevB.70.035211>.
- [24] A. Mujica, A. Rubio, A. Munoz, R.J. Needs, High-pressure phases of group-IV, III-V, and II-VI compounds, *Rev. Mod. Phys.* 75, 863 (2003); <https://doi.org/10.1103/RevModPhys.75.863>.
- [25] H.A. Ilchuk, A.I. Kashuba, R.Yu. Petrus, I.V. Semkiv, N.A. Ukrainets, Simulation the spectral dependence of the transmittance for semiconductor thin films, *Physics and Chemistry of Solid State* 21(1), 57 (2020); <https://doi.org/10.15330/pcss.21.1.57-60>.
- [26] R. Petrus, H. Ilchuk, A. Kashuba, I. Semkiv, E. Zmiiovska, Optical properties of CdTe thin films obtained by the method of high-frequency magnetron sputtering, *Funct. Mater.* 27(2), 342 (2020); <https://doi.org/10.15407/fm27.02.342>.
- [27] Y. Wu, G. Chen, Y. Zhu, W.-J. Yin, Y. Yan, M. Al-Jassim, S.J. Pennycook, LDA+U/GGA+U calculations of structural and electronic properties of CdTe: Dependence on the effective U parameter, *Computational Materials Science* 98, 18 (2015); <https://doi.org/10.1016/j.commatsci.2014.10.051>.
- [28] S.A. Pochareddy, A.P. Nicholson, A. Thiyagarajan, A. Shah, W.S. Sampath, Structural and Electronic Calculations of CdTe Using DFT: Exchange–Correlation Functionals and DFT-1/2 Corrections, *Journal of Electronic Materials* 50, 2216 (2021); <https://doi.org/10.1007/s11664-020-08720-8>.
- [29] E.V. Shah, D.R. Roy, A comparative DFT study on electronic, thermodynamic and optical properties of telluride compounds, *Computational Materials Science* 88, 156 (2014); <https://doi.org/10.1016/j.commatsci.2014.03.013>.
- [30] D. Liu, J. Feng, M. Tian, Q. Li, R. Sa, First-principles study of the stability, electronic and optical properties of CdTe under hydrostatic pressure, *Chemical Physics Letters* 764, 138272 (2021); <https://doi.org/10.1016/j.cplett.2020.138272>.
- [31] H.S. Güder, S. Gilliland, J.A. Sans, A. Segura, J. González, I. Mora, V. Muñoz, A. Muñoz, Electronic structure and optical properties of CdTe rock-salt high pressure phase, *Phys. stat. sol. (b)* 235(2), 509 (2003); <https://doi.org/10.1002/pssb.200301612>.
- [32] J.P. Perdew, K. Burke, and M. Ernzerhof, Generalized Gradient Approximation Made Simple, *Phys. Rev. Lett.* 78(7), 1396 (1997); <https://doi.org/10.1103/PhysRevLett.78.1396>.
- [33] H.J. Monkhorst and J.D. Pack, Special points for Brillouin-zone integrations, *Phys. Rev. B.*, 13(12), 5188 (1976); <https://doi.org/10.1103/PhysRevB.13.5188>.
- [34] W. Kohn and L. J. Sham, Self-Consistent Equations Including Exchange and Correlation Effects, *Phys. Rev. A* 140(4), 1133 (1965); <https://doi.org/10.1103/PhysRev.140.A1133>.
- [35] P.A. Shchepanskyi, O.S. Kushnir, V.Yo. Stadnyk, A.O. Fedorchuk, M.Ya. Rudysh, R.S. Brezvin, P.Yu. Demchenko and A.S. Krymus, Structure and optical anisotropy of $K_{1.75}(NH_4)_{0.25}SO_4$ solid solution, *Ukr. J. Phys. Opt.* 18(4), 187 (2017); <https://doi.org/10.3116/16091833/18/4/187/2017>.
- [36] M.Ya. Rudysh, P.A. Shchepanskyi, A.O. Fedorchuk, M.G. Brik, C.-G. Ma, G.L. Myronchuk, and M. Piasecki, First-principles analysis of physical properties anisotropy for the Ag_2Si_3 chalcogenide semiconductor, *Journal of Alloys and Compounds* 826(15), 154232 (2020); <https://doi.org/10.1016/j.jallcom.2020.154232>.
- [37] B. Naidych, T. Parashchuk, I. Yaremiy, M. Moyseyenko, O. Kostyuk, O. Voznyak, Z. Dashevsky, and L. Nykyruy, Structural and thermodynamic properties of Pb-Cd-Te thin films: Experimental study and DFT analysis, *Journal of Electronic Materials* 50(2), 580-591 (2021); <https://doi.org/10.1007/s11664-020-08561-5>.
- [38] O. Madelung, M. Schlz, H. Weiss (Eds.), Numerical Data and Functional Relationships in Science and Technology, Landolt-Borstein, 17 (Springer, Berlin, 1982).
- [39] A.J. Strauss, The physical properties of cadmium telluride, *Revue de Physique Appliquée, Société française de physique/EDP* 12(2), 167 (1977); <https://doi.org/10.1051/rphysap:01977001202016700>.
- [40] S. Pershyna, A. Kashuba, I. Semkiv, Ya. Storozhuk, H. Ilchuk, R. Petrus, Deposition and optical characterization of the cadmium telluride thin films, *Visnyk of the Lviv University. Series Physics* 58, 3 (2021); <https://doi.org/10.30970/vph.58.2021.3>.
- [41] D.T.F. Marple, Refractive Index of ZnSe, ZnTe, and CdTe, *J. Appl. Phys.* 35, 539 (1964); <https://doi.org/10.1063/1.1713411>.
- [42] F.B. Baghsiyahi, A. Akhtar and M. Yeganeh, Ab initio study of thermodynamic properties of bulk zinc-blende CdS: Comparing the LDA and GGA, *International Journal of Modern Physics B* 32, 1850207 (2018); <https://doi.org/10.1142/S0217979218502077>.

Г.А. Ільчук¹, Л.І. Никируй², А.І. Кашуба¹, І.В. Семків¹, М.В. Соловійов¹,
Б.П. Найдич², В.М. Кордан³, Л.Р. Дева¹, М.С. Каркульовська¹, Р.Ю. Петрусь¹

Електронні, фононні, оптичні та термодинамічні властивості кристалу CdTe, розраховані методом функціонала густини

¹Національний університет “Львівська політехніка”, вул. С.Бандери, 12, 79013 Львів, Україна, andrii.i.kashuba@lpnu.ua

²Прикарпатський національний університет імені Василя Стефаника, вул. Шевченка, 57, 76018 Івано-Франківськ, Україна, lyubotyr.nykyruy@pnu.edu.ua

³Львівський національний університет імені Івана Франка, вул. Кирила і Мефодія, 6, 79005 Львів, Україна;

Представлено результати теоретичного розрахунку електронного та фононного енергетичного спектру, оптичних і термодинамічних властивостей кристалів CdTe. Дисперсія електронного та фононного енергетичного спектру у високо симетричних точках зони Бріллюена, електронна та фононна щільність станів, температурна поведінка спектрів комбінаційного розсіювання, питомої теплоємності, вільної енергії, ентропії, ентальпії і температури Дебая розрахована в межах наближення узагальненого градієнта апроксимації з використанням функціоналу Пердью–Берк–Ернцергоф. Для аналізу оптичних функцій використано комплексну діелектричну функцію. Розраховані параметри добре корелюють із відомими експериментальними результатами.

Ключові слова: теорія функціонала густини, зонні структури, оптичні функції, термодинамічні властивості.